Role of Amino Acid Residues at Turns in the Conformational Stability and Folding of Human Lysozyme[†,‡]

Kazufumi Takano,[§] Yuriko Yamagata,[||] and Katsuhide Yutani*[,§]

Institute for Protein Research, Osaka University, Yamadaoka, Suita, Osaka 565-0871, Japan, and Graduate School of Pharmaceutical Sciences, Osaka University, Yamadaoka, Suita, Osaka 565-0871, Japan

Received December 14, 1999; Revised Manuscript Received May 5, 2000

ABSTRACT: To clarify the role of amino acid residues at turns in the conformational stability and folding of a globular protein, six mutant human lysozymes deleted or substituted at turn structures were investigated by calorimetry, GuHCl denaturation experiments, and X-ray crystal analysis. The thermodynamic properties of the mutant and wild-type human lysozymes were compared and discussed on the basis of their three-dimensional structures. For the deletion mutants, Δ47−48 and Δ101, the deleted residues are in turns on the surface and are absent in human α-lactalbumin, which is homologous to human lysozyme in amino acid sequence and tertiary structure. The stability of both mutants would be expected to increase due to a decrease in conformational entropy in the denatured state; however, both proteins were destabilized. The destabilizations were mainly caused by the disappearance of intramolecular hydrogen bonds. Each part deleted was recovered by the turn region like the α-lactalbumin structure, but there were differences in the main-chain conformation of the turn between each deletion mutant and α-lactalbumin even if the loop length was the same. For the point mutants, R50G, Q58G, H78G, and G37Q, the main-chain conformations of these substitution residues located in turns adopt a left-handed helical region in the wild-type structure. It is thought that the left-handed non-Gly residue has unfavorable conformational energy compared to the left-handed Gly residue. Q58G was stabilized, but the others had little effect on the stability. The structural analysis revealed that the turns could rearrange the main-chain conformation to accommodate the left-handed non-Gly residues. The present results indicate that turn structures are able to change their main-chain conformations, depending upon the side-chain features of amino acid residues on the turns. Furthermore, stopped-flow GuHCl denaturation experiments on the six mutants were performed. The effects of mutations on unfolding−refolding kinetics were significantly different among the mutant proteins. The deletion/substitutions in turns located in the α-domain of human lysozyme affected the refolding rate, indicating the contribution of turn structures to the folding of a globular protein.

The tertiary structures of globular proteins contain turn and/or loop structures in addition to secondary structures, the α-helix and *β*-strand (*1*). Turn structures change the polypeptide chain directions, connect the secondary structure elements, and compact the protein structures as a globule. There are conventional interests in the roles of turns in the tertiary structure, conformational stability, and folding of proteins, whether turns are no more than linkers of secondary structure elements or the turns hold the keys to the formation of tertiary structures.

To address these issues, some studies have investigated the effects of turns on the stability and folding kinetics by modifying the loop length or sequence in the turns of α-helix bundle proteins (*2*−*4*), *β*-barrel proteins (*5*−*7*), and small proteins (<100 amino acid residues) (*8, 9*). The results have shown that the role of turns in the stability and folding is strongly context-dependent (*9*). In the previous studies, however, information on the structural changes due to modification in the turns has been mostly lacking: how do modifications in the turns affect the structure? How are the stability and folding of mutant proteins affected by the structure changes? Moreover, in the case of more complex proteins (>100 amino acid residues) including other kinds of structural elements, such as an α + *β* structure (α-helix + *β*-sheet), the effects of modifying turn residues on the stability and folding have not yet been investigated systematically.

Human lysozyme has been extensively studied using its mutant proteins in our laboratory as a model protein for investigations of protein stability and folding (*10*−*26*). It has 130 residues, and the tertiary structure consists of two domains, α and *β* domains, which have four α-helices and two *β*-sheets, respectively (*27*). We then engineered mutants of the human lysozyme modified at the various turn structures to elucidate the individual role of the turn in human lysozyme and to gain a broad view of turn functions in globular proteins.

[†] This work was supported in part by Fellowships from the Japan Society for the Promotion of Science for Young Scientists (K.T.), by a grant-in-aid for special project research from the Ministry of Education, Science, and Culture of Japan (K.Y. and Y.Y.), and by the Sakabe project of TARA, University of Tsukuba (K.Y. and Y.Y.).

[‡] Coordinates have been deposited in the Protein Data Bank under PDB file names Δ47−48, 1DI4; Δ101, 1DI5; and R50G, 1DI3.

* Corresponding author: Telephone: +81-6-6879-8615. Fax: +81-6-6879-8616. E-mail: yutani@protein.osaka-u.ac.jp.

[§] Institute for Protein Research, Osaka University.

[||] Graduate School of Pharmaceutical Sciences, Osaka University.

10.1021/bi9928694 CCC: $19.00
Published on Web 06/27/2000

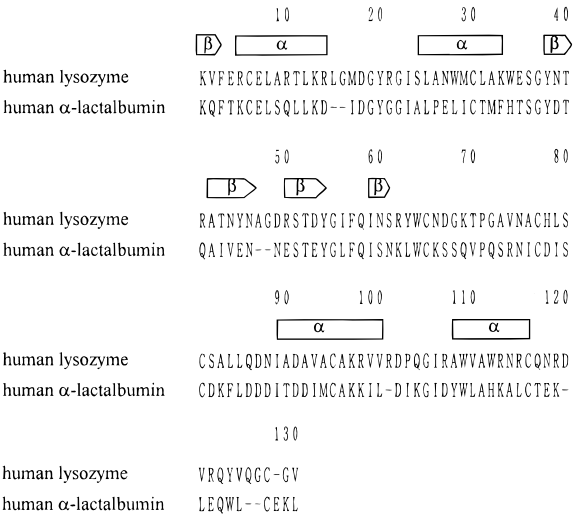

FIGURE 1: Sequence alignment of human lysozyme and human α-lactalbumin (*37*) and the corresponding secondary structure elements of human lysozyme (*27*).

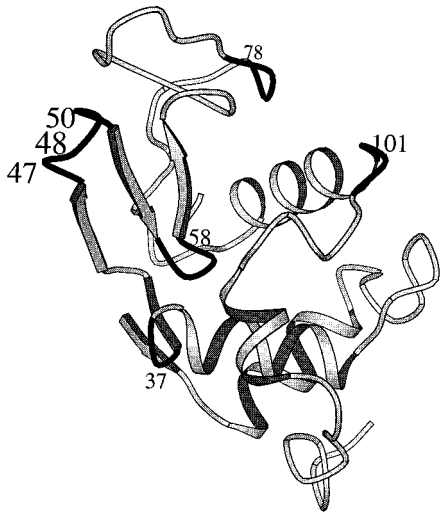

FIGURE 2: Structure of human lysozyme. The turn regions modified in this study are shown. The structure was generated with the program MOLSCRIPT (*65*).

In this study, we focused on two characteristic turn structures among various turn structures (*28, 29*). That is, (i) insertion and deletion of amino acid residues are observed in the region of turn structures more than in that of secondary structures among homologous proteins (*30, 31*) and (ii) residues with a left-handed helical configuration, having positive values of the ϕ and ψ angles, are frequently located in turn structures (*1, 32*−*34*).

Lysozyme is homologous to α-lactalbumin in amino acid sequence and tertiary structure (*35, 36*). Figure 1 shows the sequence alignment of human lysozyme and human α-lactalbumin (*37*) and the corresponding secondary structure elements of human lysozyme. In some turn regions, human lysozyme possesses extra amino acid residues, compared to human α-lactalbumin. We constructed two deletion mutants of human lysozyme, Δ47−48 and Δ101, in which the residues Ala47 and Gly48 and the residue Arg101, respectively, are deleted. The deletion residues are absent in human α-lactalbumin. The residues 47−48 are located in a turn between β-strands, and the residue 101 is located in a turn following the C-terminal end of an α-helix, as shown in Figure 2. When one or a few of the amino acid residues in a protein are eliminated, the conformational entropy in the denatured state should be decreased, providing the effects of protein stabilization.

A Ramachandran plot (*32*) of human lysozyme (*15*) is as shown in Figure 3. Most residues are in extended (around $\phi = -100°$ and $\psi = 120°$) or right-handed-helical (around $\phi = -75°$ and $\psi = -50°$) regions, but several are observed outside of the two main regions. Gly residues usually allow the outside region, but non-Gly residues are only rarely observed, due to the fact that non-Gly residues have a β-carbon. It is then thought that a left-handed non-Gly residue has unfavorable conformational energy compared to a left-handed Gly residue. We have constructed four point mutants of human lysozyme, R50G, Q58G, H78G, and G37Q (*20*). The substitution residues are located in the turn structures (Figure 2) with positive ϕ and ψ angles in the wild-type structure, so that R50G, Q58G, and H78G would be expected to increase in stability and G37Q to decrease. The residues 50, 78, and 37 are exposed to the solvent, and residue 58 is buried in the human lysozyme structure.

We characterized the stability and structures of the six human lysozyme mutants, which were deleted or substituted at the turn structures, by calorimetry, GuHCl denaturation experiments,[1] and X-ray crystal analysis. Stopped-flow GuHCl denaturation experiments of the six mutant proteins were also conducted. The effects of deletion/substitutions of amino acid residues at the turns on the conformational stability and folding of an $\alpha + \beta$ protein will be discussed on the basis of the structures of the mutant proteins.

MATERIALS AND METHODS

Mutant Proteins. Mutagenesis, expression, and purification of mutant human lysozymes examined in this study were performed as described (*15*). All chemicals were reagent grade. Protein concentration was determined spectrophotometrically using $E^{1\%}(1\text{ cm}) = 25.65$ at 280 nm (*38*).

Differential Scanning Calorimetry (DSC). Calorimetric measurements were carried out with a DASM4 microcalorimeter in 0.05 M Gly−HCl buffer at pH 2.4 to 3.3, and data analysis was done using the Origin software (MicroCal, Inc., Northampton, MA), as described (*15*). The thermodynamic parameters for denaturation as a function of temperature were calculated using the equations

$$\Delta H(T) = \Delta H(T_d) - \Delta C_p(T_d - T) \quad (1)$$

$$\Delta S(T) = \Delta H(T_d)/T_d - \Delta C_p \ln(T_d/T) \quad (2)$$

$$\Delta G(T) = \Delta H(T) - T\Delta S(T) \quad (3)$$

assuming that ΔC_p does not depend on temperature (*39*).

Equilibrium Experiment on GuHCl Denaturation. GuHCl-induced denaturation of human lysozyme was monitored by CD at 222 nm as described (*12, 23*). CD measurements were carried out with a Jasco J-720 recording spectropolarimeter using a cell of 10-mm path length and performed in 40 mM Gly−HCl buffer at pH 4.0 and 10 °C. The protein solutions

[1] Abbreviations: CD, circular dichroism; DSC, differential scanning calorimetry; GuHCl, guanidine hydrochloride.

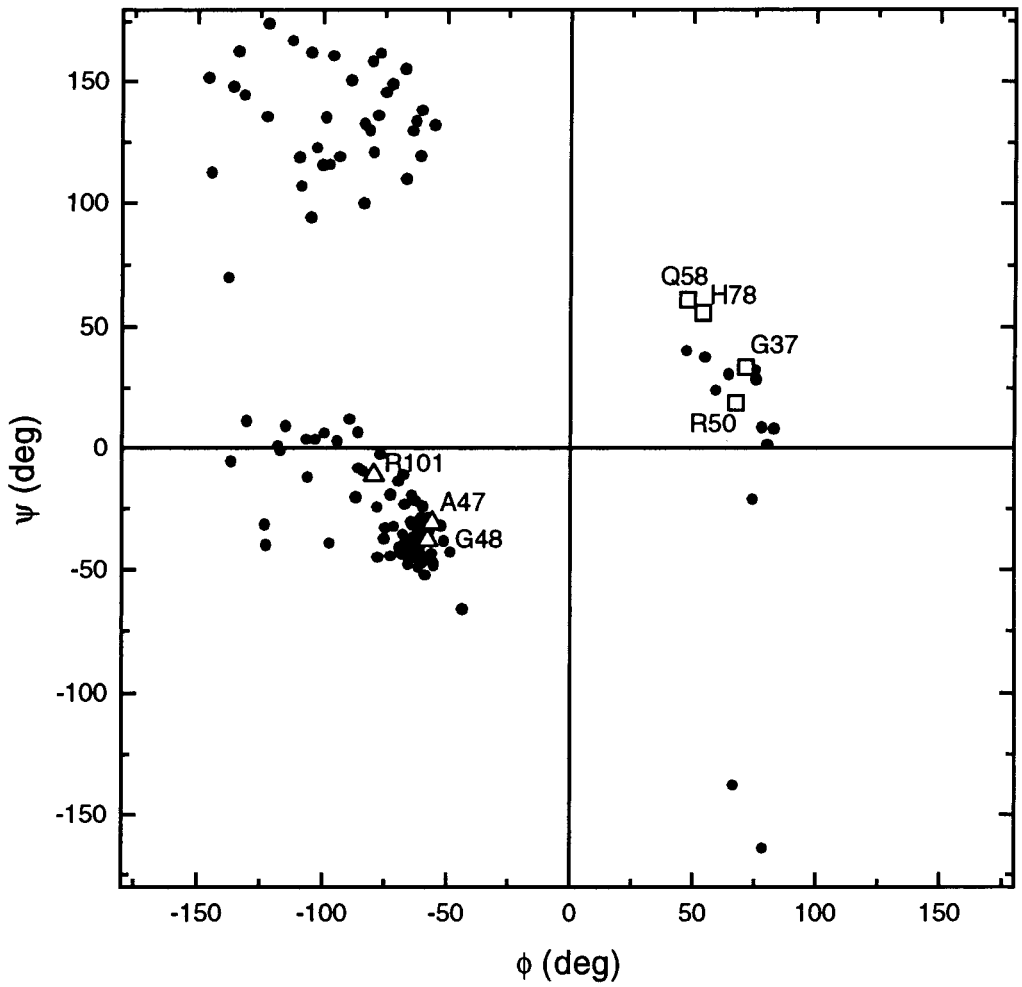

FIGURE 3: Ramachandran plot (*32*) of human lysozyme (*15*). The residues modified in this study are shown: open squares, Arg50, Gln58, His78, and Gly37; open up triangles, Ala47, Gly48, and Arg101.

were incubated for 1 day in various GuHCl concentrations at 10 °C. The fraction of unfolding (f_u) was calculated from eq 4,

$$f_u = (b_n^0 + a_n[C] - y)/(b_n^0 + a_n[C] - b_u^0 - a_u[C]) \quad (4)$$

where y is the CD value at a given GuHCl concentration, [C], and b_n^0 and b_u^0 are the CD values for the native and unfolded states at 0 M GuHCl, respectively, and a_n and a_u are the slopes of the pre- and posttransition baselines, respectively. The Gibbs energy change (ΔG) upon unfolding was calculated by the linear extrapolation model (*40*) assuming a two-state transition, according to the following equations:

$$\Delta G = -RT \ln K = -RT \ln(f_u/(1 - f_u)) \quad (5)$$

$$\Delta G = \Delta G^{H_2O} + m[C] \quad (6)$$

Here K is the equilibrium constant of the unfolding reaction and ΔG^{H_2O} and m are the Gibbs energy change upon unfolding in the absence of GuHCl and the slope of the linear correlation between ΔG and [C], respectively. f_u is then represented as a function of the GuHCl concentration as follows:

$$f_u = 1/[\,1 + \exp((\Delta G^{H_2O} + m[C])/RT)] \quad (7)$$

We used the Origin software (MicroCal, Inc., Northampton, MA) to produce a least-squares fit of the experimental data in the GuHCl unfolding curves to eq 7 in order to obtain ΔG^{H_2O}.

X-ray Crystal Analysis. Mutant human lysozymes examined in this study were crystallized as described previously (*15*, *25*). All crystals belong to the space group $P2_12_12_1$, but the cell dimensions of Δ47−48 differ from those of the wild-type and most mutant proteins (*15*−*25*). The crystal structures of Q58G, H78G, and G37Q have been already determined (*20*).

The intensity data set for the mutant human lysozymes was collected by the oscillation method on the Rigaku R-AXIS IIC imaging plate mounted on the Rigaku RU300 for Δ47−48, by synchrotron radiation at the Photon Factory (Tsukuba, Japan) on beam line 6A with a Weissenberg camera (*41*) for Δ101, and by synchrotron radiation at the SPring-8 (Harima, Japan) on beam line 41XU (Proposal No. 1999A0210-CL-np) for R50G. The data were processed with the program DENZO (*42*) for Δ101 and with the software provided by Rigaku for Δ47−48 and R50G. The structures were solved by the isomorphous method using the program X-PLOR (*43*) for Δ101 and R50G (*15*, *25*) and by the molecular replacement technique using the program AMoRe (*44*) for Δ47−48 (*24*). The structure was refined with the program X-PLOR (*43*) as described previously (*15*).

Table 1: Thermodynamic Parameters for Denaturation of Mutant Human Lysozymes at Different pH Values

	pH	T_d (°C)	ΔH_{cal} (kJ/mol)	ΔH_{vH} (kJ/mol)
Δ47−48	2.55	57.2 ± 0.0	395 ± 2	401 ± 2
	2.71	59.9 ± 0.0	402 ± 3	416 ± 4
	3.08	64.9 ± 0.0	423 ± 2	439 ± 3
Δ101	2.52	60.3 ± 0.1	407 ± 6	439 ± 5
	2.72	63.3 ± 0.1	431 ± 8	448 ± 8
	3.14	70.7 ± 0.1	460 ± 5	481 ± 4

Kinetic Experiments on GuHCl Unfolding and Refolding. The reaction of unfolding and refolding by GuHCl was monitored by the fluorescence intensity measurement above 300 nm with excitation at 280 nm as described (*12*, *23*). Fluorescence stopped-flow experiments were carried out with a Photal RA-401 stopped-flow spectrophotometer equipped with a mixing device using 1:10 volumes of two solutions (Otsuka Electronics, Osaka, Japan) and were performed in 40 mM Gly-HCl buffer at pH 4.0 and 10 °C. The protein solutions for refolding were incubated for 1 day in 5.5 M GuHCl concentrations at 10 °C. The kinetic data were fitted using the Origin software by the method of nonlinear least-squares with the following equation:

$$A(t) - A(\infty) = \sum A_i \exp(-k_i t) \quad (8)$$

Here $A(t)$ and $A(\infty)$ are the fluorescence intensities at a given time, t, and at a time when no further change is observed, respectively, A_i is the amplitude of the ith phase, and k_i is the apparent rate constant of the ith phase.

RESULTS

Equilibrium Stability of Mutant Human Lysozymes: Calorimetry and GuHCl Denaturation. To examine the changes in conformational stability of the mutant human lysozymes, we measured the heat and denaturant stability by DSC and GuHCl denaturation experiments monitored with CD, respectively.

DSC measurements for Δ47−48 and Δ101 were carried out in an acidic pH region (pH 2.5−3.2) where the heat denaturation of human lysozyme is highly reversible. Table 1 shows the denaturation temperature (T_d), the calorimetric enthalpy changes (ΔH_{cal}), and the van't Hoff enthalpy changes (ΔH_{vH}) of each measurement for the mutants. Calorimetric experiments for R50G, Q58G, H78G, and G37Q have been already investigated (*20*). Table 2 shows the thermodynamic parameters for denaturation of the mutant and wild-type proteins at the same temperature, 64.9 °C, which is the denaturation temperature of the wild-type at pH 2.7 (*15*). The results indicate that H78G, G37Q, and both deletion mutants (Δ47−48 and Δ101) were destabilized compared with the wild-type protein, but the stability of R50G and Q58G increased due to the substitutions.

Denaturation by GuHCl of the human lysozymes was monitored by CD at 222 nm as a function of the denaturant concentration at pH 4 and 10 °C, which is the same condition for the kinetic studies. The transition curves upon denaturation were highly cooperative at certain GuHCl concentrations, and the denaturation was completely reversible. The thermodynamic parameters for denaturation at pH 4 and 10 °C were calculated using eqs 5−7, as shown in Table 3. The denaturation Gibbs energies in water, ΔG^{H_2O}, of Δ47−48, Δ101, H78G, and G37Q were smaller than that of the wild-type protein, indicating the destabilization by the substitutions. In contrast, increases in stability were observed for R50G and Q58G.

Structures of Mutant Human Lysozymes. Data collection and refinement statistics for Δ47−48, Δ101, and R50G human lysozymes are summarized in Table 4. The crystal structures of Q58G, H78G, and G37Q have been already determined (*20*). The overall folded structures of the mutant human lysozymes were essentially similar to that of the wild-type protein.

The deletion residues of Δ47−48 and Δ101 are located in the turn structures near a β-strand and an α-helix, respectively, in the wild-type structure (Figures 1 and 2). The structures in the vicinity of the mutation sites for Δ47−48 and Δ101 are illustrated in Figure 4. Both deletions caused structure changes not in the secondary structures but in the turn regions. The turn regions recovered the deletion space (Figures 4a,d). The Δ47−48 structure deleted three intramolecular hydrogen bonds in total compared with the wild-type structure, as shown in Figures 4b,c. In the case of Δ101, one intramolecular hydrogen bond disappeared (Figures 4e,f).

In the Q58G, H78G, and G37Q structures, the main-chain conformations of the turns were apparently similar to that in the wild-type structure as displayed in Figure 5a−c. In contrast, the main-chain conformation of the turn between residues 47 and 50 was slightly different between the wild-type and R50G structures as shown in Figure 5d.

Kinetic Studies for Refolding−Unfolding of Mutant Human Lysozymes. To examine the effects of substitutions on the folding of the mutant human lysozymes, kinetic studies of the reversible refolding−unfolding were performed. All measurements were carried out at pH 4 and 10 °C. The refolding and unfolding reactions were monitored by fluorescence intensity. The logarithm of the apparent rate constants, k_{app}, as a function of GuHCl concentration is shown in Figure 6.

The unfolding kinetics of the mutant human lysozymes was described by a single exponential, as was reported for the wild-type protein (*12*). The k_{app} values of Δ47−48, Δ101, and H78G were higher than that of the wild-type protein, indicating the acceleration of the unfolding rate by the mutations. In the case of R50G, the unfolding rate slowed.

The refolding reactions of the mutant human lysozymes, except for Δ101, were described as two phases at low GuHCl concentrations, which is like that of the wild-type protein (*12*). The amplitude of the fast phase in the two phases observed in the refolding kinetics was greater than that of the slow phase in any case, indicating that the fast phase is predominant in the refolding reaction. Canet et al. (*45*) have reported that the refolding of human lysozyme at pH 5 and 25 °C has three phases (I−III). Phase I occurs in several milliseconds (*45*), which is within the dead time of our experiments (about 10 ms). Thus, we did not observe three phases but two phases, because of different experimental conditions or dead time. The k_{app} values for the fast phase in this study of Δ47−48, R50G, and H78G were identical to that of the wild-type protein, but the other mutants changed the refolding rates: Q58G accelerated; Δ101 and G37Q slowed.

Table 2: Thermodynamic Parameters for Denaturation of Mutant Human Lysozymes at 64.9 °C, pH 2.7

	T_d (°C)	ΔT_d (°C)	ΔC_p[a] (kJ/mol K)	ΔH (kJ/mol)	$\Delta\Delta H$ (kJ/mol)	$T\Delta\Delta S$ (kJ/mol)	$\Delta\Delta G$ (kJ/mol)
wild-type[b]	64.9 ± 0.5		6.6 ± 0.5	477 ± 4			
Δ47−48	59.5 ± 0.3	−5.4	3.7 ± 0.4	423 ± 2	−54	−48	−6.7
Δ101	63.2 ± 0.3	−1.7	4.9 ± 0.9	433 ± 7	−44	−42	−2.2
R50G[c]	65.8 ± 0.1	+0.9	6.1 ± 1.5	420 ± 10	−57	−58	+1.1
Q58G[c]	70.6 ± 0.5	+5.7	5.6 ± 0.2	455 ± 1	−22	−30	+7.8
H78G[c]	64.4 ± 0.0	−0.5	6.6 ± 0.5	455 ± 4	−22	−22	−0.5
G37Q[c]	64.1 ± 0.0	−0.8	4.8 ± 0.8	450 ± 5	−27	−26	−1.1

[a] ΔC_p was obtained from the slope of ΔH_{cal} versus T_d. [b] Takano et al. (*15*). [c] Takano et al. (*20*).

Table 3: Thermodynamic Parameters for Equilibrium Unfolding of Mutant Human Lysozymes at 10 °C and pH 4.0

	m (kJ/mol M)	C_m[a] (M)	ΔG^{H_2O} (kJ/mol)	$\Delta\Delta G^{H_2O}$ (kJ/mol)
wild-type	−15.1 ± 0.0	3.96 ± 0.01	60.0 ± 0.1	
Δ47−48	−15.2 ± 0.1	3.46 ± 0.01	52.7 ± 0.2	−7.3
Δ101	−15.1 ± 0.2	3.60 ± 0.02	54.5 ± 0.8	−5.5
R50G	−15.2 ± 0.1	4.11 ± 0.01	62.2 ± 0.2	+2.2
Q58G	−16.1 ± 0.2	4.26 ± 0.02	68.6 ± 0.8	+8.6
H78G	−15.2 ± 0.1	3.81 ± 0.01	57.8 ± 0.2	−2.2
G37Q	−14.8 ± 0.2	3.79 ± 0.02	56.4 ± 0.4	−3.6

[a] C_m is the GuHCl concentration of the midpoint in the transition.

Table 4: X-ray Data Collection and Refinement Statistics of Mutant Human Lysozymes

	Δ47−48	Δ101	R50G
	Data Collection		
space group	$P2_12_12_1$	$P2_12_12_1$	$P2_12_12_1$
cell (Å)			
a	45.80	56.42	56.28
b	59.27	61.69	62.96
c	38.91	32.86	32.46
resolution (Å)	2.0	2.2	1.8
no. of measd reflections	20 055	27 719	26 966
no. of indepdt reflcns	7155	5952	10 060
completeness (%)	94.1	97.3	90.8
R_{merge} (%)[a]	8.1	4.2	4.5
	Refinement		
no. of atoms	1198	1206	1248
no. of solvent atoms	178	188	226
resolution (Å)	8.0−2.0	8.0−2.2	8.0−1.8
no. of reflcns used	6820	5530	9573
completeness (%)	92.0	91.5	86.6
R factor[b]	0.165	0.165	0.190

[a] $R_{merge} = 100\Sigma|I - \langle I\rangle|/\Sigma\langle I\rangle$. [b] R factor $= \Sigma||F_o| - |F_c||/\Sigma|F_o|$.

DISCUSSION

Effect of Deletion at the Turn on the Structure and Stability of Human Lysozyme. It has been reported that in homologous proteins, insertion and deletion of amino acid residues occur in the region of turn/loop structures more than in that of secondary structures, the α-helix and *β*-strand (*30*, *31*). In the case of two deletion mutants of human lysozyme, Δ47−48 and Δ101, the deletion residues are located in surface turn structures near a *β*-strand and an α-helix, respectively, in the wild-type structure (Figure 2) and are absent in human α-lactalbumin that is homologous to human lysozyme in sequence and structure (Figure 1). X-ray crystal analysis of the deletion mutants revealed that the deleted space was made up of the turn regions, not the secondary structural regions, so that each turn in both structures was shortened (Figure 4), suggesting that the secondary structure regions fold independently of the turn regions. It then seems that these turn structures of human lysozyme play the role of a linker of the secondary structure elements. Sagermann et al. (*46*) have also reported that the structures of individual α-helices are determined predominantly by the nature of the amino acids within the helix rather than the structural environment provided by the rest of the protein.

When one or a few of the amino acid residues in a protein are eliminated, the conformational entropy in the denatured state should be decreased. This provides the effect of protein stabilization. Thompson and Eisenberg (*47*) have shown that thermophile proteins possess shorter amino acid lengths in the loop regions than their homologous mesophile proteins, indicating that thermophile proteins might gain the high thermostability due to turn deletions. In the case of the two deletion mutants of human lysozymes, the entropy changes ($T\Delta S$) upon denaturation of Δ47−48 and Δ101 could be estimated to be reduced by 13.7 and 3.7 kJ/mol at 65 °C, respectively, using the method by Oobatake and Ooi (*48*). However, both proteins destabilized as compared with the wild-type protein (Tables 2 and 3), indicating that the deleted residues in the turns of human lysozyme might contribute to the protein stabilization. The calorimetric experiments show that these destabilizations were caused by an enthalpic effect (Table 2). The decreases in enthalpy change observed were not overcome by the decreases in entropy change. These results mean that the deletions of human lysozyme also affected other destabilization factors in addition to the entropic effect, such as hydration effects, hydrophobic interaction, hydrogen bonds, and steric strain (conformational energy). The changes in hydration and hydrophobic effects upon mutation might be not very large, because the deletion sites are on the surface of the folded structure. On the other hand, three and one intramolecular hydrogen bonds disappeared in the Δ47−48 and Δ101 structures, respectively, due to the deletions (Figure 4). One intramolecular hydrogen bond contributes to protein stability by 8−9 kJ/mol (*21*), so that both deletion mutants of human lysozyme were mainly destabilized by the removal of hydrogen bonds. In the case of deletions at the α-helices in T4 lysozyme, the deletion mutants have been remarkably destabilized by 11.7−22.6 kJ/mol (*49*). Therefore, a deletion of amino acid residues is not always able to stabilize the protein by the entropic effect of the denatured state, because other interactions caused by the deletion compensate for the entropic effect.

Comparison between Deletion Mutants of Human Lysozyme and Human α-Lactalbumin. In the Δ47−48 and Δ101 human lysozymes, each turn which was modified has the same loop length as that in human α-lactalbumin. Figure 7 shows the structures in the vicinity of the deletion sites of Δ47−48 and Δ101, compared with those of human α-lactalbumin.

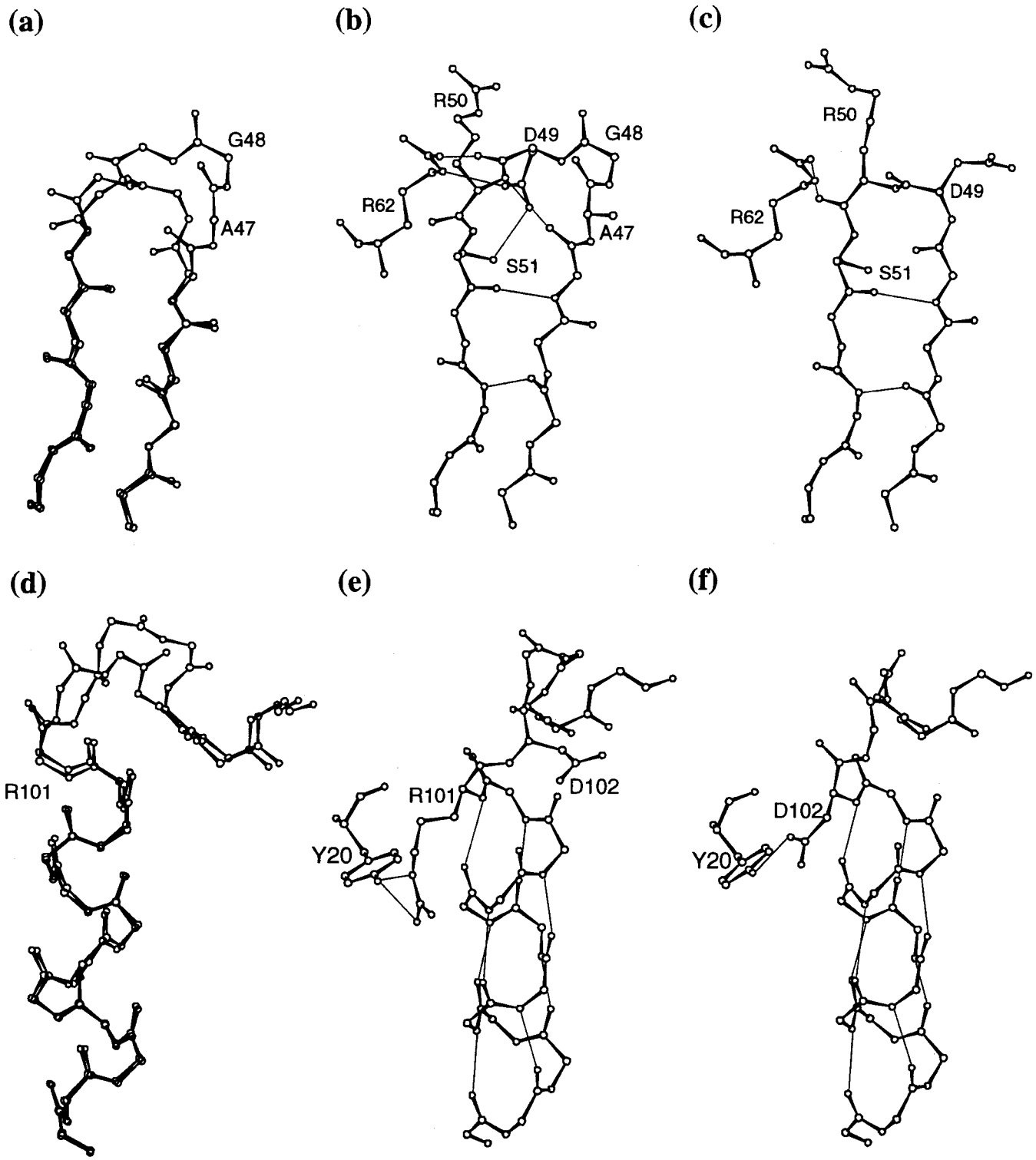

FIGURE 4: Structures in the vicinity of the mutation sites: for Δ47−48, (a) Δ47−48 and wild-type, (b) wild-type, and (c) Δ47−48; for Δ101, (d) Δ101 and wild-type, (e) wild-type, and (f) Δ101. In (a) and (d), only main-chain atoms are drawn. In (b) and (c), the side-chain atoms of Ala47, Asp49, Arg50, Ser51, and Arg62 are drawn. In (e) and (f), the side-chain atoms of Arg101, Asp102, and Tyr20 are drawn. The thin lines represent hydrogen bonds.

In the case of Δ47−48, there was a slight difference in the main-chain conformation in the part of the turn between Δ47−48 and human α-lactalbumin, although the main-chain conformation in the β-sheet in Δ47−48 was similar to that in human α-lactalbumin (Figure 7a). Each side chain of Asp49 in Δ47−48 and Asn45 in human α-lactalbumin did not interact with any other protein atoms, so that the difference in turn conformation might be caused by the difference in interaction with other amino acid residues between Arg50 in Δ47−48 and Glu46 in human α-lactalbumin. The side chain of Glu46 in human α-lactalbumin is able to hydrogen bond with a main-chain atom of the turn (Figure 7b), but that of Arg50 in Δ47−48 was not (Figure 7c). In Δ101, the turn which was modified also had a different main-chain turn conformation from that in human α-lactalbumin (Figure 7d). The amino acid sequence of the

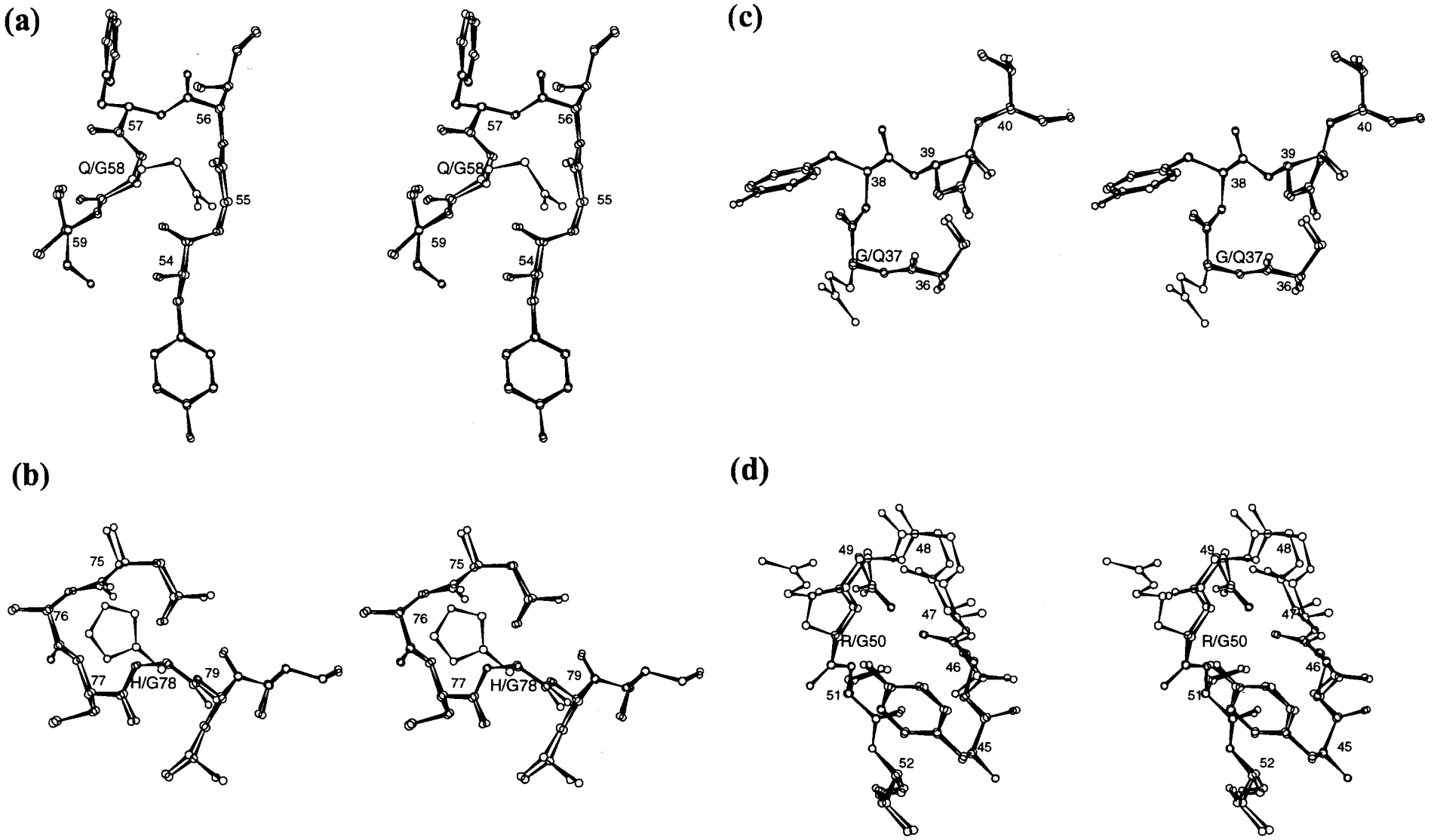

FIGURE 5: Stereodrawings of the structures in the vicinity of the mutation sites for (a) Q58G and wild-type, (b) H78G and wild-type, (c) G37Q and wild-type, and (d) R50G and wild-type (*20*). The wild-type and mutant structures are superimposed.

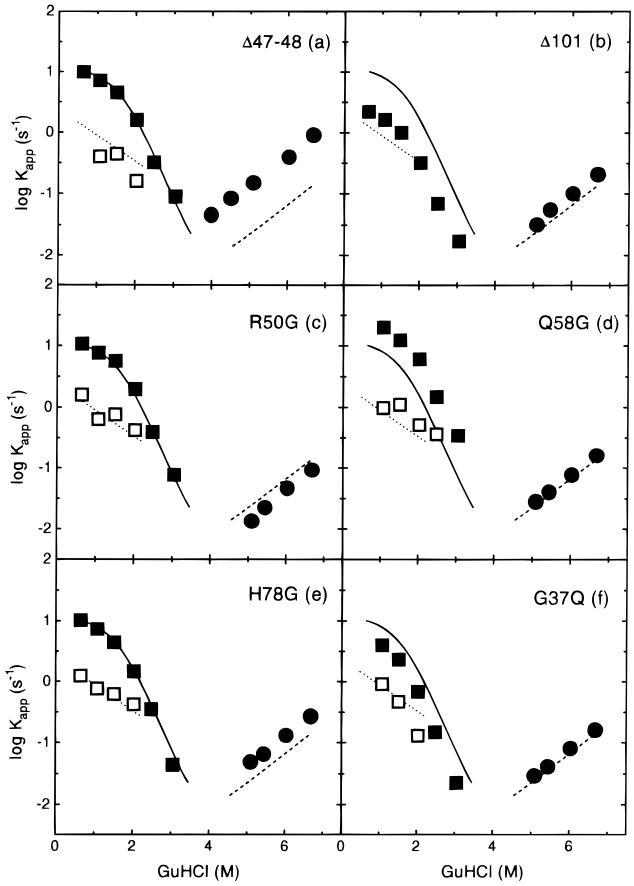

FIGURE 6: Logarithm of apparent rate constants as a function of GuHCl concentration of (a) Δ47−48, (b) Δ101, (c) R50G, (d) Q58G, (e) H78G, and (f) G37Q mutant human lysozymes. Closed circles, closed squares and open squares depict the data for unfolding, fast-phase refolding, and slow-phase refolding, respectively, of the mutant proteins. Dashed, solid, and dotted lines represent the data for unfolding, fast-phase refolding, and slow-phase refolding, respectively, of the wild-type protein.

turn in Δ101 is Asp102−Pro103−Gln104−Gly105−Ile106−, corresponding to Asp97−Ile98−Lys99−Gly100−Ile101− in human α-lactalbumin (Figure 1). The side chains of Pro103 and Gln104 in Δ101 and those of Ile98 and Lys99 in human α-lactalbumin were located on the protein surface. It might be then that the difference in amino acid sequence between Pro103−Gln104 in Δ101 and Ile98-Lys99 in human α-lactalbumin caused the different turn conformation, suggesting that the side-chain feature of the amino acid residue affects the main-chain conformation. These results indicate that turn conformation changes depending upon the amino acid sequence in the turn, even if the loop length is constant.

Effect of Substitution of a Left-Handed Residue at the Turn on the Stability and Structure of Human Lysozyme. As is well-known, the main-chain conformations of most residues in protein structures have an extended or right-handed helical region, but several have a left-handed helical region that corresponds to the positive values of ϕ and ψ angles (*50*). Gly residues in a protein take the left-handed conformations much more than non-Gly residues do, because the Gly residue lacks a β-carbon. In the wild-type human lysozyme structure, the residues of R50, Q58, H78, and G37 are located in the turn structures and are left-handed residues, having positive ϕ and ψ angles. The substitutions of non-Gly with Gly or Gly with non-Gly residues at these left-handed residues, Q58G, H78G, and G37Q, caused few structure changes (Figures 5a−c); the overall structures and the main-chain conformation in the turn region of the point mutants were seemingly similar to those of the wild-type protein, indicating that the turn structures are able to accommodate both Gly and non-Gly residues with the main-chain torsion angles of the left-handed region. Such an observation has also been reported in D30G of Rop, in which the substitution residue is left-handed at a surface turn (*3*). In the case of R50G human lysozyme, the turn conformation changed compared with that in the wild-type structure (Figure 5d). This turn structure might be more limber than the other turns, because the turn structure is on the surface of human lysozyme and includes another Gly residue at position 48 (Gly48).

It has been reported that the conformational energy of a left-handed non-Gly residue is unfavorable relative to a Gly residue with the same ϕ and ψ angles (*51*, *52*). The left-handed structure of non-Gly residue has a higher conformational energy that is caused by interaction between the β-carbon and the main chain than does the right-handed structure, by 4−8 kJ/mol (*51*−*55*). On the other hand, the destabilization effect of substitution of non-Gly for Gly residues due to an increase in main-chain conformational entropy in a denatured state is only about 1.7 kJ/mol (*56*, *57*). Therefore, the R50G, Q58G, and H78G of mutant human lysozymes would be expected to increase in stability and G37Q was expected to decrease compared with the wild-type protein, if structure changes were not introduced. However, the stability of R50G, H78G, and G37Q was essentially comparable to that of the wild-type protein, although Q58G was stabilized as expected (Tables 2 and 3).

More detailed analysis of the structures of the mutant human lysozymes revealed that the ϕ and ψ angles of the mutant structures except for R50G changed slightly, as shown in Figure 8 although the main-chain conformations around the substitution residues in Q58G, H78G, and G37Q were apparently the same as those in the wild-type structure (Figure 5). In the case of Q58G, H78G and G37Q, each Gly residue has both a larger ϕ value and a smaller ψ value than those of the corresponding non-Gly residue. These observations suggest that the turn structures changed the main-chain conformation to accommodate the left-handed non-Gly residues. The survey of left-handed Gly and non-Gly residues in protein structures has shown that non-Gly residues mostly appear in the region of $\phi = 50-70°$ and $\psi = 30-60°$, whereas Gly residues tend to have both larger ϕ values and smaller ψ values than those of non-Gly residues, reflecting each energy minimum region of non-Gly and Gly residues (*58*). Therefore, the non-Gly residues at positions 58, 78, and 37 in human lysozyme had little unfavorable energy, and the stability of H78G, and G37Q was similar to that of the wild-type protein, although Q58G was stabilized. In the case of R50G, the rearrangement of the main-chain conformation at the substituted residue as caused in Q58G, H78G and G37Q was not induced at residue 50 (Figure 8): the ϕ and ψ values of R50 are on the outside region of those of the left-handed non-Gly residues usually observed. However, the turn conformation was different between the wild-type and R50G structures, as shown in Figure 5d. Therefore, judging from the stability change upon mutation of R50G (Tables 2 and 3), the turn structure admits R50 with the support of the other residues within the turn. These results

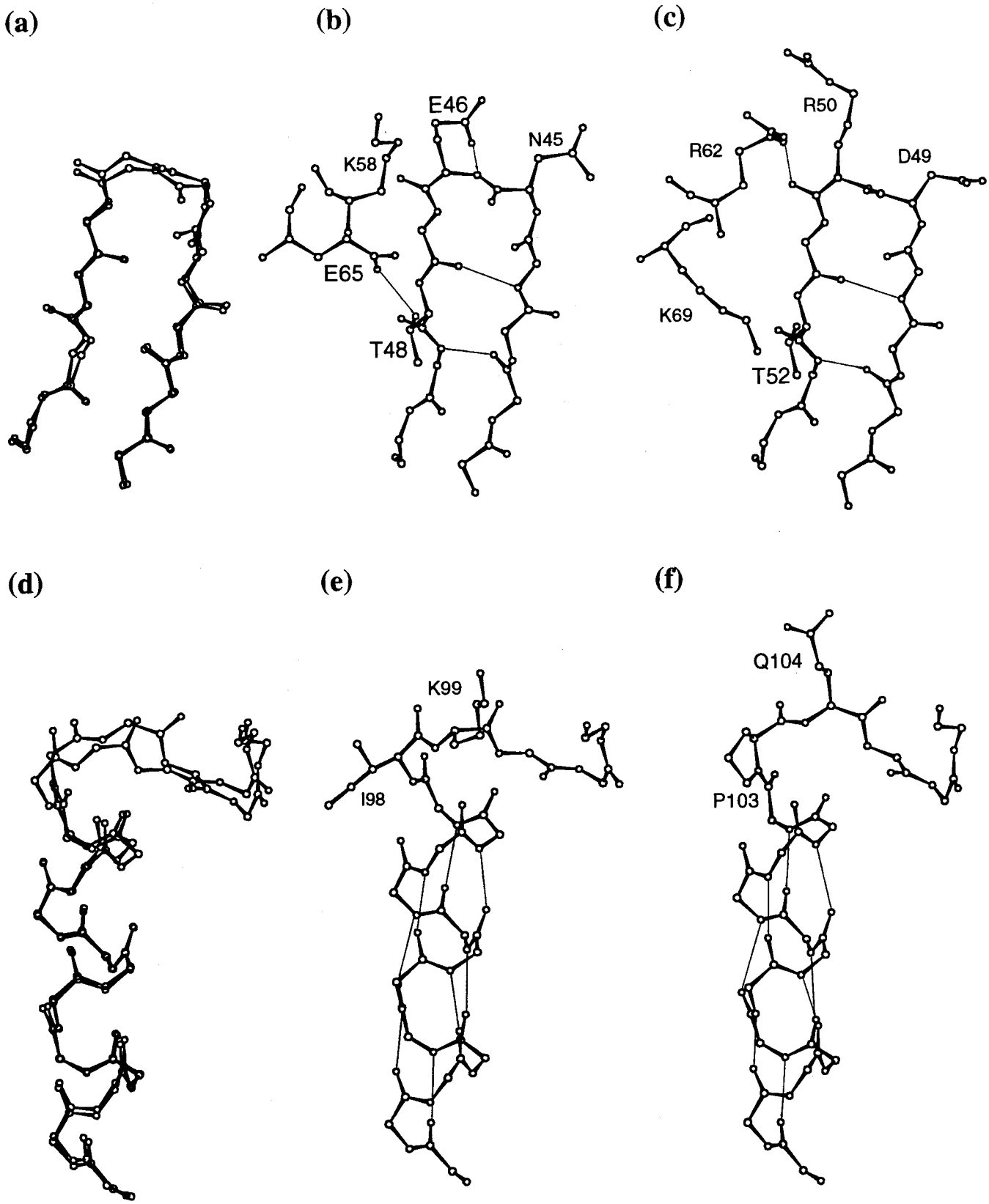

FIGURE 7: Structures in the vicinity of the mutation sites: for Δ47−48, (a) human α-lactalbumin and Δ47−48 of human lysozyme, (b) human α-lactalbumin, and (c) Δ47−48; for Δ101, (d) human α-lactalbumin and Δ101 of human lysozyme, (e) human α-lactalbumin, and (f) Δ101. In (a) and (d), only main-chain atoms are drawn. In (b), the side-chain atoms of Asn45, Glu46, Thr48, Lys58, and Glu65 are drawn. In (c) the side-chain atoms of Asp49, Arg50, Thr52, Arg62, and Lys69 are drawn. In (e), the side-chain atoms of Ile98 and Lys99 are drawn. In (f) the side-chain atoms of Pro103 and Gln104 are drawn. The thin lines represent hydrogen bonds.

show that turn structures are able to adjust their conformation to accommodate left-handed non-Gly residues without unfavorable energy.

Why was only Q58G stabilized? Q58G might be stabilized due to a decrease in the side-chain conformational entropy in the denatured state, because residue 58 is buried in the

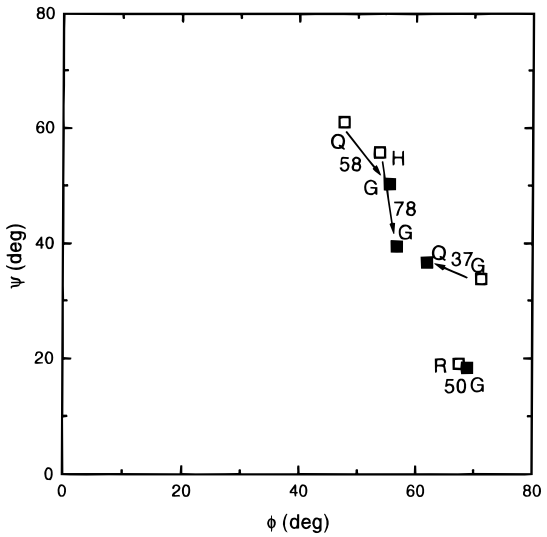

FIGURE 8: Ramachandran plot (*32*) of the residues 50, 58, 78, and 37 in the wild-type human lysozyme structure (open squares) and each mutant structure (closed squares).

native structure. On the other hand, because residues 50, 78, and 37 are exposed to the solvent, side-chain entropic effects might not occur. Pickett and Sternberg (*59*) have estimated the side-chain entropic effect of the replacement of Q by G, 8.1 kJ/mol, at 65 °C, which was comparable with the observed value of Q58G, 7.8 kJ/mol (Table 2).

Role of Turn in the Folding of Human Lysozyme. From stopped-flow GuHCl unfolding-refolding experiments, the changes in the unfolding−refolding kinetics upon deletion/substitutions of human lysozyme were significantly different, depending on the mutation sites; Δ47−48, R50G, and H78G changed the unfolding rate but had little effect on the refolding rate (fast phase), while Δ101, Q58G, and G37Q changed the refolding rate but had little effect on the unfolding rate (Figure 6).

The differences in the activation Gibbs energy changes of unfolding and refolding in water between the wild-type and mutant proteins ($\Delta\Delta G_u^{\ddagger\,H_2O}$ and $\Delta\Delta G^{\ddagger\,H_2O}$, respectively) are estimated by use of the following equations

$$\Delta\Delta G_u^{\ddagger\,H_2O} = -RT \ln[k_u^{H_2O}(\text{mutant})/k_u^{H_2O}(\text{wild})] \quad (9)$$

$$\Delta\Delta G_f^{\ddagger\,H_2O} = -RT \ln[k_f^{H_2O}(\text{mutant})/k_f^{H_2O}(\text{wild})] \quad (10)$$

where $k_u^{H_2O}$ and $k_f^{H_2O}$ are the unfolding and refolding rate constants in water, respectively. For Δ47−48, R50G, and H78G human lysozymes which did not change the refolding rate, the $-\Delta\Delta G_f^{\ddagger\,H_2O}$ values were calculated to be only −0.3, −0.2, and −0.2 kJ/mol, respectively. This means that the mutation sites are not organized in the transition state of refolding of human lysozyme (*60*−*62*). The $\Delta\Delta G_u^{\ddagger\,H_2O}$ values were also calculated to be −5.1, +2.6, and −1.6 kJ/mol, respectively. These values are equivalent to the differences in equilibrium Gibbs energy change in water ($\Delta\Delta G^{H_2O}$), −7.3, +2.2, and −2.2 kJ/mol, respectively (Table 3), indicating that the changes in stability due to the mutation are mainly interpreted in terms of the change in unfolding rate. These three mutation sites are located in the surface of the β-domain of human lysozyme. On the contrary, for Δ101, Q58G, and G37Q, the $-\Delta\Delta G_f^{\ddagger\,H_2O}$ values were calculated to be −4.4, +2.1, and −2.6 kJ/mol, respectively, but the $\Delta\Delta G_u^{\ddagger\,H_2O}$ values were calculated to be only −0.5, 0, and −0.4 kJ/mol, respectively. These results indicate that the mutation sites have been partly refolded in the transition state. The residues 101 and 37 are located in the α-domain, and residue 58 is located in the interface between the α- and β-domains. Canet et al. (*45*) have reported that the α-domain and interface between the α- and β-domains in human lysozyme fold faster than the β-domain, which coincided with the present observations. Δ47−48, R50G, and H78G which were modified in the β-domain did not influence the predominant refolding reaction, in which the α-domain mainly folds. In contrast, the refolding rate of Δ101, Q58G, and G37Q which were modified in/near the α-domain was affected, indicating that these turn structures contribute to the folding of human lysozyme.

In peptide fragments, turns contribute significantly to the stability and play an important role in the structure formation (*63*, *64*). These effects are also observed in all β-proteins; a β-barrel protein plastocyanin is not able to tolerate the turn modifications (*5*), and turns in a β-sandwich protein α-spectin SH3 domain can play a critical role in the stability and folding (*6*). In contrast, turns in α-bundle proteins do not play a dominant role in determining the folded structures (*2*, *3*), although the turn modifications influence the stability and folding (*3*, *4*). For a small protein with an α-helix and four β-strands, peptostreptococcal protein L, the two turns show the contrasting effects on the protein folding between them, indicating that turn role is strongly context-dependent (*9*). In the case of a more complex α + β globular protein, turn modifications hardly affect the tertiary/secondary structures but influence the stability and folding, depending on the location, as shown in this study. These reports suggest that because hydrophobic core is absent or scarce in peptide fragments and β-barrel proteins, the turn structures should be the main contributor of structure formation. In contrast, turn structures of α-bundle proteins and α + β globular proteins are held by several interactions such as hydrophobic interaction, resulting in that a turn in globular proteins would tolerate the various modifications and affect the protein folding in many ways, depending on the site.

CONCLUSION

In this study, we could show the role of turns in the conformational stability, structure, and folding of a protein using six mutant human lysozymes, which are deleted or substituted at turn structures. The mutations are expected to stabilize the proteins; shortening the turn on the protein surface stabilizes due to entropic effect, and substitution of non-Gly for a Gly at the left-handed region does due to removal of unfavorable steric interactions. The obtained results were, however, contrary to the expectations. The deletion mutants were destabilized by the structural changes due to mutation; the loss of some hydrogen bonds caused the unexpected loss in stability. The structural analysis also revealed that each turn region had the same loop length as that in the homologous α-lactalbumin structure; that is, each part deleted was recovered by the remainder of the turn region, suggesting that a turn structure is able to tolerate the loop length modification. The stability of Gly mutants, R50G, H78G, and G37Q, substituted on the surface hardly changed, but that for one case at a buried site, Q58G, was stabilized. These data do not support the opinion that the substitution

of a non-Gly residue for a Gly residue at the left-handed region always stabilizes the protein. The structural data showed that turn structures could accommodate left-handed non-Gly residues without unfavorable energy by adjustments in the main-chain conformations. The stabilization at the buried site might be due to the effect of side-chain entropy. Consequently, the variability of turn conformation should be considered for engineering a turn as one wishes, but the tolerance of a turn against a modification would provide the potentiality for engineering.

ACKNOWLEDGMENT

We thank Takeda Chemical Ind., Ltd. (Osaka, Japan), for providing plasmid pGEL125.

REFERENCES

1. Richardson, J. S. (1981) *Adv. Protein Chem. 34*, 167−339.
2. Brunet, A. P., Huang, E. S., Huffine, M. E., Loeb, J. E., Robert, J. W., and Hecht, M. H. (1993) *Nature 364*, 355−358.
3. Predki, P. F., Agrawal, V., Brunger, A. T., and Regan, L. (1996) *Nat. Struct. Biol. 3*, 54−58.
4. Nagi, A. D., Anderson, K. S., and Regan, L. (1999) *J. Mol. Biol. 286*, 257−265.
5. Ybe, J., and Hecht, M. (1996) *Protein Sci. 5*, 814−824.
6. Martinez, J. C., Pisabarro, M. T., and Serrano, L. (1998) *Nat. Struct. Biol. 5*, 721−729.
7. Kim, K., and Frieden, C. (1998) *Protein Sci. 7*, 1821−1828.
8. Zhou, H., Hoess, R. H., and DeGrado, W. F. (1996) *Nat. Struct. Biol. 3*, 446−450.
9. Gu, H. D., Kim, D., and Baker, D. (1997) *J. Mol. Biol. 274*, 588−596.
10. Herning, T., Yutani, K., Taniyama, Y., and Kikuchi, M. (1991) *Biochemistry 30*, 9882−9891.
11. Herning, T., Yutani, K., Inaka, K., Kuroki, R., Matsushima, M., and Kikuchi, M. (1992) *Biochemistry 31*, 7077−7085.
12. Taniyama, Y., Ogasahara, K., Yutani, K., and Kikuchi, M. (1992) *J. Biol. Chem. 267*, 4619−4624.
13. Kuroki, R., Inaka, K., Taniyama, Y., Kidokoro, S., Matsushima, M., Kikuchi, M., and Yutani, K. (1992) *Biochemistry 31*, 8323−8328.
14. Kuroki, R., Kawakita, S., Nakamura, H., and Yutani, K. (1992) *Proc. Natl Acad. Sci. U.S.A. 89*, 6803−6807.
15. Takano, K., Ogasahara, K., Kaneda, H., Yamagata, Y., Fujii, S., Kanaya, E., Kikuchi, M., Oobatake, M., and Yutani, K. (1995) *J. Mol. Biol. 254*, 62−76.
16. Takano, K. Yamagata, Y., Fujii, S., and Yutani, K. (1997) *Biochemistry 36*, 688−698.
17. Takano, K., Funahashi, J., Yamagata, Y., Fujii, S., and Yutani, K. (1997) *J. Mol. Biol. 274*, 132−142.
18. Takano, K., Yamagata, Y., and Yutani, K. (1998) *J. Mol. Biol. 280*, 749−761.
19. Takano, K., Yamagata, Y., Kubota, M., Funahashi, J., Fujii, S., and Yutani, K. (1999) *Biochemistry 38*, 6623−6629.
20. Takano, K., Ota, M., Ogasahara, K., Yamagata, Y., Nishikawa, K., and Yutani, K. (1999) *Protein Eng. 12*, 663−672.
21. Takano, K., Yamagata, Y., Funahashi, J., Hioki, Y., Kuramitsu, S., and Yutani, K. (1999) *Biochemistry 38*, 12698−12708.
22. Takano, K., Tsuchimori, K., Yamagata, Y., and Yutani, K. (1999) *Eur. J. Biochem. 266*, 675−682.
23. Funahashi, J., Takano, K., Ogasahara, K., Yamagata, Y., and Yutani, K. (1996) *J. Biochem. 120*, 1216−1223.
24. Funahashi, J., Takano, K., Yamagata, Y., and Yutani, K. (1999) *Protein Eng. 12*, 841−850.
25. Yamagata, Y., Kubota, M., Sumikawa, Y., Funahashi, J., Takano, K., Fujii, S., and Yutani, K. (1998) *Biochemistry 37*, 9355−9362.
26. Kuroki, R., and Yutani, K. (1998) *J. Biol. Chem. 273*, 34310−34315.
27. Artymiuk, P. J., and Blake, C. C. F. (1981) *J. Mol. Biol. 152*, 737−762.
28. Lewis, P. N., Momany, F. A., and Scheraga, H. A. (1973) *Biochim. Biophys. Acta 303*, 211−229.
29. Oliva, B., Bates, P. A., Querol, E., Aviles, F. X., and Sternberg, M. J. E. (1997) *J. Mol. Biol. 266*, 814−830.
30. Thornton, J. M. (1990) *Nature 343*, 411−412.
31. Sibanda, B. L., and Thornton, J. M. (1991) *Methods Enzymol. 202*, 59−82.
32. Ramachandran, G. N., Ramakrishnan, C., and Sasisekharan, V. (1963) *J. Mol. Biol. 7*, 95−99.
33. Rose, G. D., Gierasch, L. M., and Smith, J. A. (1985) *Adv. Protein Chem. 37*, 1−109.
34. Thornton, J. M., Sibanda, B. L., Edwards, M. S., and Barlow, D. J. (1988) *BioEssays 8*, 63−69.
35. Brew, K., Vanaman, T. C., and Hill, R. L. (1967) *J. Biol. Chem. 242*, 3747−3749.
36. McKenzie, H. A., and White, F. H., Jr. (1991) *Biochem. Int. 14*, 347−356.
37. Sugai, S., and Ikeguchi, M. (1994) *Adv. Biophys. 30*, 37−84.
38. Parry, R. M., Chandan, R. C., and Shahani, K. M. (1969) *Arch. Biochem. Biophys. 130*, 59−65.
39. Privalov, P. L., and Khechinashvili, N. N. (1974) *J. Mol. Biol. 86*, 665−684.
40. Pace, C. N. (1986) *Methods Enzymol. 131*, 266−280.
41. Sakabe, N. (1991) *Nucl. Instr. Methods Phys. Res. A303*, 448−463.
42. Otwinowski, Z. (1990) DENZO data processing package, Yale University, New Haven, CT.
43. Brunger, A. T. (1992) *X-PLOR Manual*, Ver. 3.1, Yale University, New Haven, CT.
44. Navaza, J. (1994) *Acta Crystallogr. A50*, 157−163.
45. Canet, D., Sunde, M., Last, A. M., Miranker, A., Spencer, A., Robinson, C. V., and Dobson, C. M. (1999) *Biochemistry 38*, 6419−6427.
46. Sagermann, M., Baase, W. A., and Matthews, B. W. (1999) *Proc. Natl Acad. Sci. U.S.A. 96*, 6078−6083.
47. Thompson, M. J., and Eisenberg, D. (1999) *J. Mol. Biol. 290*, 595−604.
48. Oobatake, M., and Ooi, T. (1993) *Prog. Biophys. Mol. Biol. 59*, 237−284.
49. Vetter, I. R., Baase, W. A., Heinz, D. W., Xiong, J. P., Snow, S., and Matthews, B. W. (1996) *Protein Sci. 5*, 2399−2415.
50. Ramachandran, G. N., and Sasisekharan, V. (1968) *Adv. Protein Chem. 23*, 283−437.
51. Stites, W. E., Meeker, A. K., and Shortle, D. (1994) *J. Mol. Biol. 235*, 27−32.
52. Kimura, S., Kanaya, S., and Nakamura, H. (1992) *J. Biol. Chem. 267*, 22014−22017.
53. Zimmerman, S. S., Pottle, M. S., Nemethy, G., and Scheraga, H. A. (1977) *Macromolecules 10*, 1−9.
54. Weiner, S. J., Kollmann, P. A., Case, D. A., Singh, U. C., Ghio, C., Alagona, G., Profeta, S., Jr., and Weiner, P. (1984) *J. Am. Chem. Soc. 106*, 765−784.
55. Head-Gordon, T., Head-Gordon, M., Frisch, M. J., Brooks, C. L. I., and Pople, J. A. (1991) *J. Am. Chem. Soc. 113*, 5989−5997.
56. Nemethy, G., Leach, S. J., and Scheraga, H. A. (1966) *J. Phys. Chem. 70*, 998−1004.
57. Matthews, B. W., Nicholson, H., and Becktel, W. (1987) *Proc. Natl. Acad. Sci. U.S.A. 84*, 6663−6667.
58. Nicholson, H., Soderlind, E., Tronrud, D. E., and Matthews, B. W. (1989) *J. Mol. Biol. 210*, 181−193.
59. Pickett, S. D., and Sternberg, M. J. (1993) *J. Mol. Biol. 231*, 825−839.
60. Kuwajima, K., Mitani, M., and Sugai, S. (1989) *J. Mol. Biol. 206*, 547−561.
61. Matouschek, A., Kellis, J. T., Jr., Serrano, L., and Fersht, A. R. (1989) *Nature 340*, 122−126.
62. Serrano, L., Matouschek, A., and Fersht, A. R. (1992) *J. Mol. Biol. 224*, 805−818.
63. Dyson, H. J., Rance, M., Houghten, R. A., Lerner, R. A., and Wright, P. E. (1998) *J. Mol. Biol. 201*, 161−200.
64. Milburn, P. J., Konishi, Y., Meinwald, Y. C., and Scheraga, H. A. (1987) *J. Am. Chem. Soc. 109*, 4486-4496.
65. Kraulis, P. J. (1991) *J. Appl. Crystallogr. 24*, 946−950.

BI9928694